characteristic of the particular topology of the ligand cat-30. This very slow decomplexation process via either of the two possible paths is in good agreement with a recent crystallographic study of both Cu(cat-30)$^+$ and its free ligand cat-30.[23] The molecular structures of the two compounds are very different. In the catenate, the two diphenylphenanthroline subunits are held in close proximity by complexation to Cu(I), forming a relatively compact assembly due to the interlacing of the dpp fragments, whereas they are fully separate after decomplexation, being far apart one from the other. The kinetic catenand effect is thus directly related to the difficulty encountered by the two rings in disengaging from a given molecular arrangement, while remaining interlocked during the unravelling process. The molecular structure of Cu(cat-30)$^+$ shows that the coordination polyhedron of Cu^I is so distorted with respect to a tetrahedron that the metal center is relatively accessible to small ligands.[23] In fact, the steric hindrance around the copper atom is not significantly greater in Cu(cat-30)$^+$ than in Cu(dap)$_2$$^+$. The observed kinetic stabilization of the cuprocatenate with respect to acyclic analogues is thus entirely due to the special topology of the ligand.

In summary, the present results show that the decomplexation reaction rates of various copper(I) complexes span a wide range. Whereas the least hindered complex, Cu(dmp)$_2$$^+$, dissociates rapidly under given conditions (in the order of 0.1 s), the entwining of two phenanthroline ligands bearing aromatic groups α to the nitrogen atoms leads to a special molecular topography, greatly decreasing the rate of the demetalation process ($\sim$1 s). The introduction of rings to the molecules and, in particular, their interlocking around the copper atom induces an additional decrease in demetalation rate. The resulting catenand effect leads to kinetically inert complexes: the disentangling of two interlocked macrocyclic ligands during the decomplexation process requires a complete disengagement of the molecule while maintaining interlocking of the rings. Dissociation of the cuprocatenate or of strained monocyclic complexes is therefore a slow reaction ($\sim$10^3 s).

(23) Cesario, M.; Dietrich-Buchecker, C. O.; Guilhem, J.; Pascard, C.; Sauvage, J. P. *Chem. Commun.* **1985**, 244.

Ground-State Analogues of Transition States for Attack at Sulfonyl, Sulfinyl, and Sulfenyl Sulfur: A Sulfuranide Dioxide (10-S-5) Salt, a Sulfuranide Oxide (10-S-4) Salt, and a Sulfuranide (10-S-3) Salt[1]

C. W. Perkins, S. R. Wilson, and J. C. Martin*

Contribution from the Roger Adams Laboratory, Department of Chemistry, University of Illinois, Urbana, Illinois 61801. Received June 18, 1984. Revised Manuscript Received December 3, 1984

Abstract: The preparation and properties of anionic 10-S-5, 10-S-4, and 10-S-3 species (**1**, **2**, and **3**) are described. The X-ray crystallographic structures show these species to be pseudotrigonal bipyramidal in geometry in the solid state. Data from pK_a measurements and low-temperature NMR spectra prove the importance of hypervalent bonding in the ground-state structures in solution as well. The anions of **1** and **2** are the first examples of sulfuranide dioxide and sulfuranide oxide anions. They are also shown to be hypervalent in the solution phase. The anions of **1**, **2**, and **3** are shown by measurements of pK_a values for their open-chain conjugate acids (7.2, 5.0, and 4.4, respectively) to be at least 2.6, 5.9, and 7.5 kcal/mol more stable than their open-chain isomers. The results of X-ray crystallographic studies of these anions are discussed, as well as the implications that the isolation and characterization of these salts have on the mechanisms of associative nucleophilic displacements at sulfur.

Anions of 10-S-5 salt **1**, 10-S-4 salt **2**, and 10-S-3 salt **3** are
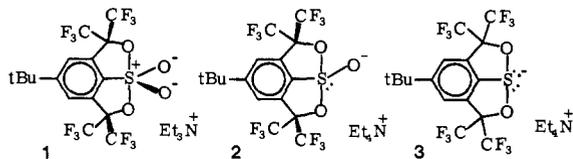
analogues of high-energy intermediates or transition states that lie along the pathway of associative nucleophilic attack at sulfonyl, sulfinyl, and sulfenyl sulfur. We call them sulfuranide dioxides, sulfuranide oxides, and sulfuranides, respectively. (In the preliminary account[1b] of this research the three species were called

sulfurandioxides, sulfuranoxides, and sulfuranides.)

In associative nucleophilic displacements, bond making and bond breaking may occur stepwise (addition–elimination) or in synchrony (no intermediate). Researchers have studied nucleophilic displacements at sulfonyl,[2] sulfinyl[3] and sulfenyl[4] sulfur in

(1) (a) The *N*-X-L designation (e.g., 10-S-3) refers to a molecule in which *N* electrons are involved in bonding *L* ligands to the central atom, X: Perkins, C. W.; Martin, J. C.; Arduengo, A. J.; Lau, W.; Alegria, A.; Kochi, J. K. *J. Am. Chem. Soc.* **1980**, *102*, 7753. (b) For a preliminary account of this work, see: Perkins, C. W.; Martin, J. C. *Ibid.* **1983**, *105*, 1377.

(2) (a) Rogne, O. *J. Chem. Soc. B* **1971**, 1855. (b) Rogne, O. *J. Chem. Soc., Perkin Trans. 2* **1972**, 472. (c) Vizgert, R. V. *Russ. Chem. Rev.* **1963**, *32*, 1. (d) Aberlin, M. E.; Bunton, C. A. *J. Org. Chem.* **1970**, *35*, 1825. (e) Graafland, T.; Wagenaar, A.; Kirby, A. J.; Engberts, J. B. F. N. *J. Am. Chem. Soc.* **1979**, *101*, 6981. (f) Laird, R. M.; Spence, M. J. *J. Chem. Soc. B* **1971**, 454. (g) Laird, R. M.; Spence, M. J. *Ibid.* **1971**, 1434. (h) Haughton, A. R.; Laird, R. M.; Spence, M. J. *J. Chem. Soc., Perkin Trans. 2* **1975**, 637. (i) Deacon, T.; Farrar, C. R.; Sikkel, B. K.; Williams, A. *J. Am. Chem. Soc.* **1978**, *100*, 2525. (j) Strangeland, L. J.; Senatore, L.; Ciuffarin, E. *J. Chem. Soc., Perkin Trans 2* **1972**, 852. (k) Hartley, B. S. *Biochem. J.* **1970**, *119*, 805. (l) Graafland, T. Ph.D. Thesis, University of Groningen, Groningen, The Netherlands. (m) Ciuffarin, E.; Sentore, L.; Isola, M. *J. Chem. Soc., Perkin Trans. 2* **1972**, 468. (n) Rogne, O. *Ibid.* **1975**, 1486. (o) Laleh, A.; Ranson, R.; Tillett, J. G. *Ibid.* **1980**, 610. (p) Kaiser, E. T. *Acc. Chem. Res.* **1970**, 145.

3210 *J. Am. Chem. Soc., Vol. 107, No. 11, 1985*

*Perkins, Wilson, and Martin*

Scheme I

Scheme II
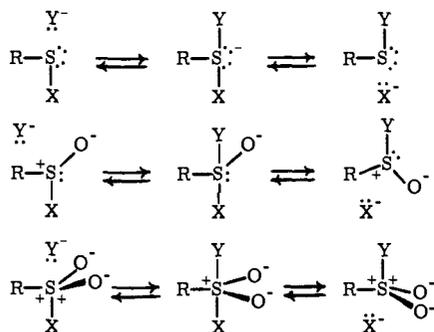
attempts to make possible a choice between synchronous and stepwise pathways. These studies have provided a wealth of information about the charge buildup on various atoms in the transition state. There have been many determinations and comparisons of ρ values,[2a-k,3c,d,4e-i] Brønsted parameters,[2a-l,3d,4b,j,k] and other parameters[2m,n,4a,b] derived from kinetic data. While these studies have met with varying degrees of success in providing reliable data from which one can infer the degree of bond making or breaking in the transition state, they have not been able to provide direct evidence for or against intermediates.

No evidence was obtained for oxygen-18 incorporation into sulfinate esters[3a,b] or sulfonate esters[2o,p] competitive with their hydrolysis in water-[18]O. Oxygen-18 incorporation observed in hydrolysis of carboxylate esters[5] has, in contrast, provided direct evidence generally interpreted in terms of a tetrahedral intermediate. Because of the usual geometric preferences of entering and leaving groups in trigonal-bypyramidal (TBP) intermediates coupled with suspected pseudorotation barriers, there is reason to expect no [18]O incorporation, even if there is an intermediate in an associative displacement at sulfur.[2o,p,6]

The fact that two sets of products result from attack of hypochlorite ion on phenyl phenylsulfinyl sulfone (4) is obviously the result of at least two reaction pathways. This was explained[3e] by suggesting that the product mixture (10% 7 and 8 from SS cleavage, and 90% 6 from OCl cleavage) results from the
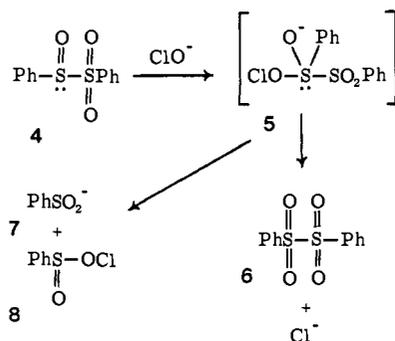
breakdown of intermediate 5 by two competitive pathways. The

two sets of products must be formed via two transition states of similar energy, but these two transition states are not necessarily preceeded by a high-energy intermediate. The direct reaction of 4 and hypochlorite ion by nucleophilic attack on the hypochlorite oxygen, via the 10-O-2 transition state (9), would lead to 6 and
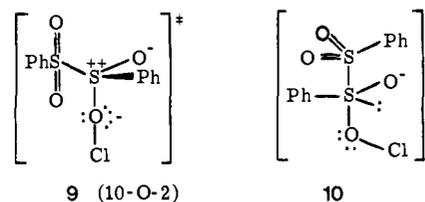
Cl⁻. The pathway through the pseudo-trigonal-bipyramidal (ψ-TBP) 10-S-4 transition state (10) would lead to 7 and 8. The S–O–Cl angle in 9 is 180°, while that in 10 is bent.

As illustrated in Scheme I substitutions at sulfenyl, sulfinyl, and sulfonyl sulfur all begin and end with tetrahedral (Td) or pseudotetrahedral (ψ-Td) bonding patterns around the central sulfur and proceed through either transition states or intermediates with TBP or ψ-TBP geometries around central sulfur. Previous success at stabilizing ψ-TBP transition state analogues for other organononmetallic species[7] prompted the synthesis of 1–3 in order to determine whether the ψ-TBP structures (analogous to those that would be high-energy intermediates or transition states along the reaction pathways discussed here) could be stabilized sufficiently, by the choice of appropriate ligands, to exist as ground-state structures.

(3) (a) Bunton, C. A.; de la Mare, P. D. B.; Greaseley, P. M.; Llewellyn, D. R.; Pratt, N. H.; Tillett, J. G. *J. Chem. Soc.* **1958**, 4751. (b) Najam, A. A.; Tillett, J. G. *J. Chem. Soc., Perkin Trans. 2* **1975**, 858. (c) Biasotti, J. B.; Andersen, K. K. *J. Am. Chem. Soc.* **1971**, *93*, 1178. (d) Senatore, L.; Ciuffarin, E.; Fava, A.; Levita, G. *Ibid.* **1973**, *95*, 2918. (e) Kice, J. L.; Puls, A. R. *Ibid.* **1977**, *99*, 3455.

(4) (a) Ciuffarin, E.; Giancarlo, G. *J. Org. Chem.* **1970**, *35*, 2006. (b) Senatore, L.; Ciuffarin, E.; Sagramora, L. *J. Chem. Soc. B* **1971**, 2191. (c) Ciuffarin, E.; Griselli, F. *J. Am. Chem. Soc.* **1970**, *92*, 6015. (d) Ciuffarin, E.; Senatore, L. *J. Chem. Soc. B* **1970**, 1680. (e) Brown, C.; Hogg, D. R. *J. Chem. Commun.* **1967**, 38. (f) Kice, J. L.; Anderson, J. M. *J. Org. Chem.* **1968**, *33*, 3331. (g) Ciuffarin, E.; Fava, A. *Prog. Phys. Org. Chem.* **1968**, *6*, 81. (h) Bosscher, J. K.; Klooasterziel, H. *Recl. Trav. Chim. Pays-Bas* **1970**, *89*, 402. (i) Boldyrev, V. G.; Kolesnikova, S. A. *J. Org. Chem. USSR (Engl. Transl.)* **1969**, *5*, 1071. (j) Ciuffarin, E.; Senatore, L.; Isola, M. *J. Chem. Soc. B* **1971**, 2187. (k) Senatore, L.; Ciuffarin, E.; Fava, A. *J. Am. Chem. Soc.* **1970**, *92*, 3035.

(5) Bender, M. L. *J. Am. Chem. Soc.* **1951**, *73*, 1626.

(6) Kice, J. L. *Adv. Phys. Org. Chem.* **1980**, *17*, 127–130, 140–145, 158–165.

(7) Martin, J. C. *Science (Washington, D.C.)* **1983**, *221*, 509.

Experimental Section

General Remarks. Chemical shifts are reported as parts per million downfield from tetramethylsilane (^{1}H) or CFCl$_3$ (^{1}F). Chemical shifts are reported in parts per million downfield from water for ^{17}O. Elemental analyses were within 0.4% of the values calculated for the listed elements. The X-ray crystallographic analyses were done by Scott Wilson in the University of Illinois X-ray Crystallographic Laboratory.

6-*tert*-Butyl-2,2-dimethyl-4,4-bis(trifluoromethyl)-4*H*-3,1-benzoxathiin (12). To a 0 °C solution of 2 mL of concentrated H$_2$SO$_4$, 25 mL of H$_2$O, 75 mL of acetonitrile, and 9.39 g (30 mmol) of amino alcohol 11[8] (see Scheme II), 2.08 g (30 mmol) of NaNO$_2$ were added in small portions over 5 min with stirring. After 3 h this solution was added dropwise to a stirred solution of S$_8$, 1.2 g (30 mmol) of NaOH, 7.8 g (32 mmol) of Na$_2$S·9H$_2$O and 15 mL of H$_2$O at 0 °C. After 4 h the resulting solution was slowly acidified (pH 1). The yellow precipitate was filtered and added to 40 mL of ethanol, 30 mL of H$_2$SO$_4$, 250 mL of H$_2$O, and 0.05 mol of powdered zinc. This mixture, after boiling for 12 h, was extracted with 3 × 150 mL of toluene. Acetone (100 mL) and *p*-toluenesulfonic acid (~2 g) were added to the toluene solution and the mixture was boiled for 6 h until only the ^{19}F singlet (−73.5 ppm) of 12 was observed in the ^{19}F NMR spectrum. Water was collected in a Dean-Stark trap. The toluene was extracted with 200 mL of 0.1 M aqueous NaOH and twice with 300 mL of H$_2$O. The water layer was extracted with 3 × 300 mL of ether. The organic layers were combined and washed with water, and solvents were removed in vacuo. Fractional distillation of the crude product resulted in a small forerun boiling at 48–54 °C. The next fraction (7.8 g, 70%) was a yellow liquid, oxathiane 12: bp 76 °C, 0.8 torr, d^{25} 1.23 g/mL; ^{1}H NMR (CDCl$_3$) δ 7.7 (br s, 1 Ar H), 7.4 (d of d, 1, Ar H), 7.2 (d, 1, Ar H), 1.7 (s, 6, CH$_3$), 1.3 (s, 9, CCH$_3$); ^{19}F NMR (CDCl$_3$) δ −73.5 (s, CF$_3$). Anal. (C$_{16}$H$_{18}$F$_6$OS) C, H, S.

6-*tert*-Butyl-2,2-dimethyl-8-[2,2,2-trifluoro-1-hydroxy-1-(trifluoromethyl)ethyl]-4,4-bis(trifluoromethyl)-4*H*-3,1-benzoxathiin (13). Tetramethylethylenediamine (TMEDA) (79 mL, 0.52 mol) in 300 mL of hexane was added dropwise with stirring to 239 mL (0.52 mol of 2.2 M *n*-butyllithium in hexane). After 1 h, oxathiane 12 (151 mL, 0.50 mol) in 80 mL of dry ether was added dropwise at −15 °C. After 6 h at 25 °C, the gas obtained by warming 72 mL (0.63 mol) of hexafluoroacetone (HFA) (condensed at −78 °C) was bubbled into the solution at −15 °C. **Caution:** Close attention was required to prevent even this wide-diameter tube from clogging during the addition of HFA. A −78 °C condensor was kept above the mixture while it was stirred for 5 h at 25 °C. After the mixture was shaken with 1000 mL of 2 M aqueous HCl and dried (MgSO$_4$), solvents were removed to leave an oil: ^{19}F NMR δ −73.5 (s, 1, CF$_3$ of 12), −72.7 (s, 3 CF$_3$ of 13), −74.1 (s, 3 CF$_3$ of 13). This is consistent with a mixture of 25% of 12, and 75% of 13. The oil was chromatographed on 2000 g of silica, using pentane as an eluant. After all the 12 was eluted, the column was eluted with CH$_2$Cl$_2$ until 188 g (0.35 mol, 69%) of product 13 was collected. Recrystallization from hexane gave yellow crystals of 13: mp 73–74 °C; ^{1}H NMR (CDCl$_3$) δ 7.8 (br s, 2, Ar H), 6.6 (s, 1, OH), 1.7 (s, 6, CH$_3$), 1.4 (s, 9, C(CH$_3$)$_3$); ^{19}F NMR (CDCl$_3$) δ −72.7 (s, 6, CF$_3$), −74.9 (s, 6, CF$_3$); ^{13}C NMR (CDCl$_3$, ^{1}H decoupled) δ 29.2 (s, SC(CH$_3$)$_2$O), 30.8 (s, C(CH$_3$)$_3$), 35.0 (s, C(CH$_3$)$_3$), 77.3 (septet, J_{CF} = 31 Hz, C(CF$_3$)$_2$), 81.8 (septet, J_{CF} = 31 Hz, C(CF$_3$)$_2$), 82.3 (s, s, C(CF$_3$)$_2$O), 128.0 (d, ArCH), 128.4 (s, Ar C), 131.5 (s, Ar CS), 149.2 (s, Ar CC(CH$_2$)$_3$); mass spectrum (10 eV), *m/z* (relative intensity) 538 (50, M$^+$·), 523 (100, M$^+$· − CH$_3$), 465 (24, M$^+$· − 2CH$_3$, C(O)CH$_3$). Anal. (C$_{19}$H$_{18}$F$_{12}$O$_2$S) C, H, S.

5-*tert*-Butyl-7-[2,2,2-trifluoro-1-hydroxy-1-(trifluoromethyl)ethyl]-3,3-bis(trifluoromethyl)-3*H*-2,1-benzoxathiole 1-Oxide (Sultine 14). A solution of 13 (63.5 g, 0.12 mol) in 650 mL of 80% v/v CH$_3$CN/H$_2$O was added dropwise to 80 g (0.449 mol) of *N*-bromosuccinimide (NBS) in the same solvent. After 20 h at 25 °C, excess aqueous Na$_2$SO$_3$ and 1 L of CCl$_4$ were added. Solvents were removed from the organic layer in vacuo. Shaking the residue with a mixture of aqueous K$_2$CO$_3$ and CCl$_4$ resulted in a precipitate that was collected by filtration. The aqueous layer was acidified and extracted with ether. The precipitate was dissolved in the ether layer, washed with aqueous HCl and dried (MgSO$_4$), and ether was removed to give 58.5 g (0.12 mol, 99%) of solid 14. Recrystallization from CH$_2$Cl$_2$/hexane gave white crystals: mp 203–205 °C; ^{1}H NMR (CD$_3$COCD$_3$) δ 8.1 (s, 2 Ar H), 5.6 (s, 1, OH), 1.4 (s, 9, CH$_3$); ^{19}F NMR (25 °C, 84 Hz, CDCCl$_3$), δ −74.5 (q, 6 J_{FF} = 9 Hz, CF$_3$), −75.9 (q, 6, J_{FF} = 9 Hz, CF$_3$); ^{19}F NMR (−50 °C, 338, MHz, CD$_3$COCD$_3$) δ −74.4 (br s, 3, CF$_3$), −74.6 (br s, 3, CF$_3$), −74.9 (br s, 3, CF$_3$), −75.9 (br s, 3, CF$_3$); ^{13}C NMR (−80 °C, CD$_3$COCD$_3$, ^{1}H decoupled) δ 28.6 (s, C(CH$_3$)$_3$), 34.4 (s, C(CH$_3$)), 76.0 (septet, J_{CF} = 30 Hz, C(CF$_3$)$_2$), 88.1 (septet, J_{CF} = 32 Hz, C(CF$_3$)$_2$), 119.5 (q, J_{CF} = 285 Hz, CF$_3$), 119.9 (q, J_{CF} = 285 Hz, CF$_3$), 120.8 (q, J_{CF} = 288 Hz,

CF$_3$), 121.2 (q, J = 288 Hz, CF$_3$), 123.0 (Ar C), 127.1 (s, Ar C), 128.9 (Ar C), 130.8 (Ar C), 144.6 (s, CSO$_2$R), 157.7 (s, C-5); mass spectrum (10 eV), *m/z* (relative intensity) 512 (31, M$^+$·), 497 (100, M$^+$· − CH$_3$). Anal. (C$_{16}$H$_{12}$F$_{12}$O$_3$S) C, H.

Tetraethylammonium Salt of 4-*tert*-Butyl-1-hydroxy-2,2,6,6-tetrakis-(trifluoromethyl)-8λ^4-[1,2]oxathiolo[4,3,2-*hi*][2,1]benzoxathiole (Sulfuranide Oxide Salt 2). A solution of 14 (512 mg, 1 mmole) in 50 mL of ether was stirred with 50 mL of aqueous Et$_4$NOH for 30 min. The ether solution was dried (MgSO$_4$). White crystals of 2 (610 mg, 0.96 mmol, 96%) were obtained by slow evaporation: mp 172–173 °C; ^{1}H NMR (CD$_3$COCD$_3$) δ 7.8 (s, 2, Ar H), 3.5 (q, 8, J_{HH} = 7 Hz, CH$_2$), 1.5 (s, 9, C(CH$_3$)$_3$), 1.4 (t, 12, J_{HH} = 7 Hz, NCCH$_3$); ^{19}F NMR (25 °C, 338 MHz, CD$_3$COCH$_3$) δ −74.3 (q, 6, J_{FF} = 9 Hz, CF$_3$), −75.7 (q, 6, J_{FF} = 9 Hz, CF$_3$); ^{19}F NMR (−90 °C, 338, MHz, CD$_3$CODC$_3$) δ 74.4 (br m, 6, CF$_3$), −75.5 (br m, 6, CF$_3$); ^{13}C NMR (CD$_3$COCD$_3$, ^{1}H decoupled) δ 7.2 (s, N(CH$_2$CH$_3$)$_4$), 30.9 (s, C(CH$_3$)$_3$), 35.5 (s, C(CH$_3$)$_3$), 52.5 (s, N(CH$_2$CH$_3$)$_4$), 82.8 (septet, J_{CF} = 29 Hz, C(CF$_3$)$_2$), 123.9 (q, J_{CF} = 288 Hz, CF$_3$), 124.2 (q, J_{CF} = 288 Hz, CF$_3$) 124.4 (d, Ar CH), 137.5 (s, Ar CC(CF$_3$)$_2$OH), 146.1 (s, Ar CS), 157.4 (s, Ar CC(CH$_3$)$_3$); ^{17}O NMR (CH$_3$CN) δ 162.7 (s, 1, SO), 116.7 (s, 2 COS); FAB mass spectrum, anionic *m/z* (relative intensity) 511 (M$^+$·). Anal. (C$_{24}$H$_{31}$F$_{12}$NO$_3$S) C, H, N.

5-*tert*-Butyl-7-[2,2,2-trifluoro-1-hydroxy-1-(trifluoromethyl)ethyl]-3,3-bis(trifluoromethyl)-3*H*-2,1-benzoxathiole 1,1-Dioxide (Sulfone Alcohol 15). A solution of 14 (5.12 g, 10 mmol) and *m*-chloroperbenzoic acid (MCPBA) (5.3 g, 32 mmol) in 40 mL of *tert*-butyl alcohol was boiled for 8 h. Solvent was removed and the residue was mixed with aqueous K$_2$CO$_3$ and ether. The ether layer was dried (MgSO$_4$), and solvent was removed. The resulting solid was recrystallized from ether/hexane to give 4.78 g (9 mmol, 90%) of pure 15: mp 202–204 °C; ^{1}H NMR δ 8.0 (br s, 1, Ar H), 7.8 (br s, 1, Ar H), 1.4 (s, 9, C(CH$_3$)$_3$); ^{19}F NMR (CDCl$_3$) δ −75.0 (s, 6, CF$_3$), −75.4 (s, 6, CF$_3$); ^{19}F NMR (338 MHz, −70 °C; CD$_3$COCD$_3$) δ −74.9 (s, 6, CF$_3$), −75.5 (s, 6 CF$_3$); ^{19}F NMR (84 MHz, 0.66 equiv of C$_6$H$_5$N, CD$_3$COCD$_3$) δ 75.2 (br s, 12, CF$_3$); ^{19}F NMR (84 MHz, 10 equiv of TfOH, CH$_2$Cl$_2$) δ 75.0 (s, 6, CF$_3$), 75.4 (s, 6, CF$_3$); ^{13}C NMR (CD$_3$COCD$_3$, H decoupled) δ 30.9 (s, C(CH$_3$)$_3$), 36.7 (s, C(CH$_3$)$_3$), 78.9 (septet, J_{CF} = 31 Hz, C(CF$_3$)$_2$), 81.9 (septet, J_{CF} = 33 Hz, C(CF$_3$)$_2$), 121.7 (q, J_{CF} = 286 Hz, CF$_3$), 123.4 (q, J_{CF} = 289, CF$_3$), 125.1 (s, Ar C), 129.5 (s, Ar C), 130.8 (s, Ar C), 131.1 (s, Ar C), 159.6 (s, Ar CS), 161.5 (s, Ar CC(CH$_3$)$_3$); ^{17}O NMR δ 202 (s, 3, SO$_2$), 142 (s, COS), 0 (s, 1, COH); mass spectrum (10 eV), *m/z* (relative intensity) 528 (2, M$^+$·) 513 (100, M$^+$· − CH$_3$), 459 (3, M$^+$ − CF$_3$). Anal. (C$_{16}$H$_{12}$F$_{12}$O$_4$S) C, H.

Tetraethylammonium Salt of 4-*tert*-Butyl-1-hydroxy-1-oxo-2,2,6,6-tetrakis(trifluoromethyl)-8λ^6-[1,2]oxathiolo[4,3,2-*hi*][2,1]benzothiole (Sulfuranide Dioxide 1). A solution of 15 (528 mg, 1 mmol) in 50 mL of ether, was stirred with 50 mL of aqueous Et$_4$NOH. Slow evaporation of the ether from the dried (MgSO$_4$) solution gave 630 mg (0.96 mmol, 95%) of 1: mp 196–196.5 °C; ^{1}H NMR (CD$_3$COCD$_3$) δ 7.9 (s, 2 Ar H), 3.5 (q, 8, J_{HH} = 7 Hz, CH$_2$), 1.5 (s, 9, C(CH$_3$)$_3$), 1.4 (t, 12, CH$_3$); ^{19}F NMR (25 °C, 338 MHz, CD$_3$COCD$_3$) δ 74.9 (s, 12, CF$_3$); ^{19}F NMR (−90 °C, J = 338 MHz, CD$_3$COCD$_3$) δ −74.9 (s, 12, CF$_3$); ^{13}C NMR (CD$_3$COCD$_3$, ^{1}H decoupled) δ 7.7 (s, N(CH$_2$CH$_3$)$_4$ δ 30.9 (s, C(CH$_3$), 35.8 (s, C(CH$_3$)$_3$), 53.1 (s, N(CH$_2$CH$_3$)$_4$), 79.0 (septet, J_{CF} = 30 Hz, C(CF$_3$)$_2$), 124.5 (q, J_{CF} = 288 Hz, CF$_3$), 125.1 (s, Ar CH), 134.1 (s, Ar C, C(CF$_3$)$_2$OR), 135.3 (s, Ar CS), 160.1 (s, Ar CC(CH$_3$)$_3$); FAB mass spectrum (anionic), *m/z* 528 (M$^-$·). Anal. (C$_{24}$H$_{31}$F$_{12}$NO$_4$S) C, H, F, N, S.

2,6-Bis[1-hydroxy-1-(trifluoromethyl)-2,2,2-trifluoroethyl]-4-*tert*-butylbenzenethiol. To a stirred solution of LiAlH$_4$ (3.2 g, 84 mmol) a solution of 14 (12 g, 23 mmol) in 120 mL of ether was added dropwise. After 12 h at 25 °C, dropwise addition of 20 mL of 25% CH$_3$OH/ether was followed by dropwise addition of 10 mL of 1 M aqueous HCl. Extraction with ether, drying (MgSO$_4$), and removal of ether gave 8.6 g (17 mmol, 74%) of 16. Recrystallization from cyclohexane gave white crystals: mp 106–107 °C; ^{1}H NMR (CDCl$_3$) δ 7.9 (s, 2, Ar H), 5.9 (br s, 3, SH + OH), 1.3 (s, 9, CH$_3$); ^{19}F NMR (CDCl$_3$) δ 73.3 (s, 12, CF$_3$); ^{13}C NMR (CD$_3$COCD$_3$) δ 30.2 (s, C(CH$_3$)$_3$), 33.7 (s, C(CH$_3$)), 82.2 (septet, J_{CF} = 29 Hz, C(CF$_3$)$_2$O), 123.8 (q, J = 289 Hz, CF$_3$), 127.0 (d, Ar CH), 128.9 (s, Ar CC(CF$_3$)$_2$O), 142.0 (s, Ar CS), 143.6 (Ar CC-(CH$_3$)); mass spectrum (10 eV), *m/z* (relative intensity) 498 (28, M$^+$·), 496 (51, M$^+$· − 2H), 483 (16, M$^+$· − CH$_3$), 451 (100, M$^+$· − CH$_3$, S), 427 (40, M$^+$· − CF$_3$, 2H). Anal. (C$_{16}$H$_{14}$F$_{12}$O$_2$S) C, H, S, F.

3,3-Bis(trifluoromethyl)-5-*tert*-butyl-7-(1-hydroxy-1-(trifluoromethyl)-2,2,2-trifluoroethyl)-3*H*-2,1-benzoxathiole (Sultene 17). After 30 min at 25 °C a solution of 16 (1 g, 2 mmol), Br$_2$ (320 mg, 2 mmol), and pyridine (350 mg, 4.5 mmol) in 25 mL of CH$_2$Cl$_2$ was washed twice with aqueous HCl. The organic layer was dried (MgSO$_4$), and solvent was removed in vacuo to give 912 mg (1.84 mmol, 92%) of 17. Recrystallization from hexane gave yellow crystals: mp 161.162.5 °C; ^{1}H

---

(8) Amey, R. L. Ph.D. Thesis, University of Illinois, Urbana, IL, 1979.

NMR (CDCl$_3$) δ 7.6 (br s, 2, Ar H), 1.4 (s, 9, C(CH$_3$)); ^{19}F NMR (25 °C, 84 MHz, ether/tetrahydrofuran (THF)) δ −75.9 (br s, 6 CF$_3$), −76.3 (br s, 6, CF$_3$); ^{19}F NMR (−70 °C, 84 MHz, ether/THF) δ −75.3 (s, 6, CF$_3$), −76.2 (s, 6, CF$_3$); ^{17}O NMR (CH$_3$CN) δ 20 (s, 2, OH + COS). Anal. (C$_{16}$H$_{12}$F$_{12}$O$_2$S) C, H.

Tetraethylammonium 4-*tert*-Butyl-2,2,6,6-tetrakis(trifluoromethyl)-8λ^4-[1,2]oxathiolo[4,3,2-*hi*][2,1]benzoxathiol-8-ide (Sulfuranide 3). A solution of 1 g of **16** (2 mmol), 320 mg of Br$_2$ (4 mmol), and 360 mg of pyridine (4.5 mmol) in 25 mL of CH$_2$Cl$_2$ stood for 0.5 h at 25 °C. Washing with aqueous HCl, aqueous Et$_4$NOH, and brine and removal of CH$_2$Cl$_2$ gave **3** (1.15 g, 1.85 mmol, 92%). Recrystallization from cyclohexane and then ether/pentane gave transparent crystals of **3**: mp 180–181 °C; ^{1}H NMR (CDCl$_3$) δ 7.43 (s, 2, Ar H), 3.28 (q, 8, J_{HH} = 7 Hz, CH$_2$), 1.32 (s, 9, C(CH$_3$)$_3$), 1.30 (t, 12, J_{HH} = 7 Hz, CH$_3$); ^{13}F NMR (CDCl$_3$) δ 76.4 (s, 12, CF$_3$); ^{19}F NMR (−92 °C, 338 MHz, CD$_3$CODC$_3$) δ −76.4 (s, 12, CF$_3$); ^{13}C NMR δ 8.4 (s, N CH$_2$CH$_3$), 31.7 (s, C(CH$_3$)$_3$), 35.2 (s, C(CH$_3$)$_3$), 46.4 (s, NCH$_2$CH$_3$), 83.0 (septet, J_{CF} = 29 Hz, C(CF$_3$)$_2$), 124.7 (q, J_{CF} = 289 Hz, CF$_3$), 124.3 (s, Ar CH), 126.8 (s, Ar CC(CF$_3$)$_2$O), 143.1 (s, Ar CS), 150.2 (s, Ar CC(CH$_3$)$_3$); ^{17}O NMR (CH$_3$CN) 75.5 (s, COS); FAB mass spectrum, anionic (relative intensity), m/z 495 (M⁻·). Anal. (C$_{16}$H$_{31}$F$_{16}$O$_2$S) C, H, N.

Crystal data of 1: C$_{24}$H$_{31}$H$_{12}$NO$_4$S, 657.56, triclinic; a = 10.334 (4) Å, b = 15.247 (6) Å, c = 9.636 (4) Å, α = 95.05 (3)°, β = 91.96 (3)°, γ = 76.42 (3)°, V = 1470 (1) Å^3, Z = 2, ρ_{calcd} = 1.485 g cm^{-3}, μ(Mo Kα) = 2.08 cm^{-1}, $F(000)$ = 676.0, no conditions limiting possible reflections. Successful refinement confirmed the choice of the centrosymmetric space group $P\bar{1}$.[9]

The crystals of **1** were obtained by slowly cooling a saturated solution of **1** from chloroform/hexane. The size of the selected crystal was ca. 0.20 × 0.43 × 0.73 mm. Reflections from the ±h,±k,+l hemisphere were collected from 3.0° < 2θ < 50.0° with variable scan rates from 2.0 to 29.3 deg min^{-1} and a scan range from 0.9° below the calculated $K_{\alpha 1}$ peak position to 1.0° above the $K_{\alpha 2}$ peak position. Out of a possible 5200 unique intensities measured, 3472 were considered "observed" at the 3σ(I) level of confidence. Only these data were used during refinement. The data were corrected for Lorentz and polarization effects, empirically corrected for secondary extinction,[10a] and numerically corrected for absorption.[10b] The refined isotropic extinction coefficient converged to a value of 2.0 (10) × 10^{-7}; maximum and minimum transmission factors for the absorption correction were 0.96 and 0.89, respectively.

Solution and Refinement of Structure 1. The structure was solved by direct methods (MULTAN[10c]); correct positions for 30 of the 42 non-hydrogen atoms were deduced from an E map. A weighted difference Fourier map with contributions from these 30 atoms revealed positions for the 12 remaining non-hydrogen atoms. Subsequent least-squares–difference Fourier calculations[10d] failed to yield positions for all of the hydrogen atoms; consequently, positions were calculated for all hydrogens on the basis of chemically reasonable geometry, tetrahedral or trigonal planar, with an assumed bond length of 0.95 Å. In the final cycle of least-squares refinement, positions for all non-hydrogen atoms were varied with anisotropic thermal coefficients, an empirical isotropic extinction coefficient was refined, and the hydrogen atoms were fixed in calculated positions; the maximum change/error was 0.002. The function minimized was $\sum||F_o| - |F_c||^2$, where F_o and F_c are the observed and calculated structure factors, respectively. Refinements converged to conventional agreement factors of R_1 = 0.046 and R_2 = 0.060 ($R_1 = ||F_o| - |F_c||/\sum|F_o|$; $R_2 = [\sum\omega||F_o| - |F_c||^2/\sum\omega|F_o|^2]^{1/2}$. The final difference Fourier map had three peaks with densities greater than background but was otherwise featureless. These peaks were situated in a tetrahedral arrangement about the central carbon atom of the *tert*-butyl moiety at an average distance of 1.58 Å. Refinement of a molecular model accounting for this disorder did not improve the fit of the data, so these low-percentage disordered carbon atoms were not included in the refinement scheme. There were no apparent systematic errors in the final observed and calculated structure factors. Positional parameters, calculated hydrogen positions, thermal parameters, observed and calculated

structure factors, and a complete list of bond lengths and angles are available as supplementary material.

Crystal Data of 2: C$_{24}$H$_{31}$F$_{12}$NO$_3$S, M_r 641.56, triclinic; a = 10.463 (4) Å, b = 15.241 (6) Å, c = 9.550 (4) Å, α = 95.18 (3)°, β = 92.48 (3)°, γ = 76.17 (3)°, V = 1472 (1) Å^3, Z = 2, ρ_{calcd} = 1.447 g cm^{-3}, μ(Mo K$_\alpha$) = 2.03 cm^{-1}, $F(000)$ = 660.0. No conditions limited possible reflections. Successful refinement confirmed the choice of the centrosymmetric space group $P\bar{1}$.[9]

The crystals of **2** were obtained by slow evaporation of solvent from a saturated ether/pentane solution. The size of the selected crystal was ca. 0.38 × 0.4 × 0.48 mm. Reflections from the ±h,±k,+l hemisphere were collected from 3.0° < 2θ < 50.0° with variable scan rates from 2.0 to 29.3 deg min^{-1} and a scan range from 0.8° below the calculated $K_{\alpha 1}$ peak position to 0.9° above the $K_{\alpha 2}$ position. Out of a possible 6800 unique intensities measured, 3043 were considered "observed" at the 3σ(I) level of confidence. Only those data were used during refinement. The data were corrected for Lorentz and polarization effects but not for secondary extinction or absorption.

Solution and Refinement of the Structure of 2. The structure was solved by correlation with molecule **1**. Since the two molecules crystallized in the same space group with nearly equal cell edges, the coordinates determined from the first structure were simply refined with the new data and cell parameters.[10d] In the final cycle of least-squares refinement, positions for all non-hydrogen atoms (except O3 and O3′) were refined with anisotropic thermal coefficients. Positions and a site occupancy factor were refined for the two disordered oxygen atoms with a common isotropic thermal coefficient. An isotropic group thermal parameter was refined for hydrogen atoms fixed in idealized positions. The site occupancy factor for atom O3 converged to a value of 0.828 (5). The maximum change/error in the last cycle was 0.003. Refinement converged to conventional agreement factors of R_1 = 0.058 and R_2 = 0.078. The final difference Fourier map showed a minor disorder around the central *tert*-butyl carbon atom but was otherwise featureless. There were no apparent systematic errors in the final observed and calculated structure factors. Positional parameters, calculated hydrogen positions, thermal parameters, observed and calculated structure factors, and a complete list of bond lengths and angles are available as supplementary material.

Crystal Data of 3: C$_{24}$H$_{31}$F$_{12}$NO$_2$S, M_r 625.56, monoclinic, a = 18.600 (6) Å, b = 11.495 (4) Å, c = 13.446 (5) Å, β = 99.34 (3)°, V = 2937 (2) Å, Z = 4, ρ_{calcd} = 1.464 g cm^{-3}, μ(Cu K$_\alpha$) = 19.40 cm^{-1}, $F(000)$ = 1288.0. Systematic absences for hkl, $h + k = 2n + 1$, suggested three possible space groups, $C2$, C_m, $C2/m$. Successful refinement confirmed the choice of centrosymmetric space group $C2/m$.[9]

The crystals of **3** were obtained by slow evaporation of solvent from a saturated ether/pentane solution. The size of the selected crystal was ca. 0.33 × 0.55 × 0.68 mm. Reflections from the +h,+k,±l quadrant were collected from 2.0° < 2θ < 140.0° with variable scan rates from 2.0 to 19.6 deg min^{-1} and a scan range from 0.9° below the calculated K$_{\alpha 1}$ peak position to 1.1° above the K$_{\alpha 2}$ position. Out of a possible 2553 unique intensities measured, 2131 were considered "observed" at the 3σ(I) level of confidence. Only these data were used during refinement. The data were collected for Lorentz and polarization effects, empirically corrected for secondary extinction,[10a] and numerically corrected for absorption.[10b] The refined isotropic extinction coefficient converged to a value of 4 (3) × 10^{-7}; maximum and minimum transmission factors for the absorption correction were 0.602 and 0.303, respectively.

Solution and Refinement of 3. The structure was solved with direct methods (MULTAN[10c]); correct positions for 21 of the 31 non-hydrogen atoms were deduced from an E map. A weighted difference Fourier map revealed positions for the lone remaining non-hydrogen atom for the anion and the central nitrogen atom from the cation. Subsequent least-squares–difference Fourier calculations[10d] gave positions for eight carbon atoms of the cation disordered about the mirror plane. In the final cycle of least squares, positions for all non-hydrogen atoms were refined with anisotropic thermal coefficients, an empirical isotropic extinction parameter was refined, and the hydrogen atoms of the anion were fixed in idealized positions with a variable isotropic group thermal parameter. The hydrogen atoms of the cation were not included in the final structure factor calculation. The maximum change/error for the last cycle was 0.15; conventional agreement factors of R_1 = 0.074 and R_2 = 0.116 were obtained. The final difference Fourier map had five peak maxima above background; all five were located in the vicinity of the anion and the maximum density was 0.41 e Å^{-3}. There were no significant systematic errors in the observed and calculated structure factors. Positional parameters, calculated hydrogen positions, thermal parameters, observed and calculated structure factors, and a complete list of bond lengths and angles are available as supplementary material.

Measurement of pK_a Values of 14, 15, and 16. The fluoro alcohols [ca. 10 mL of 1.0 × 10^{-2} M solutions in 70% (v/v) ethanol/water] were

(9) The cell parameters were obtained at 25 °C by a least-squares fit to the automatically centered settings for 15 reflections on a Syntex P2$_1$ automated diffractometer equipped with a graphite monochromator (Mo K$\bar{\alpha}$) λ = 0.710 69 Å or (Cu K$\bar{\alpha}$) λ = 1.541 78 Å. Intensity data were measured at 25 °C on the same instrument in the 2θ–θ scan mode with stationary crystal–stationary counter backgrounds counted at either end of the scan range for 12.5% of the total scan time per reflection. Three standard intensities were monitored for every 100 reflections.

(10) (a) Zachariasen, W. H. *Acta Crystallogr.* **1963**, *16*, 1139. (b) Busing, W. R.; Levy, H. A. *Ibid.* **1957**, *10*, 180. (c) Main, P.; Fiske, S. J.; Hull, S. E.; Lessinger, L.; Germain, G.; Declercq, J.-P.; Woolfson, M. M. MULTAN 80, a system of computer programs for the automatic solution of crystal structures from X-ray diffraction data, 1980. (d) Sheldrick, G. M. SHELX 76, a program for crystal structure determination, 1976.

Ground-State Analogues of Transition States

J. Am. Chem. Soc., Vol. 107, No. 11, 1985 3213

Scheme III

14a ⇌ 14b

15a ⇌ 15b

17a ⇌ 17b
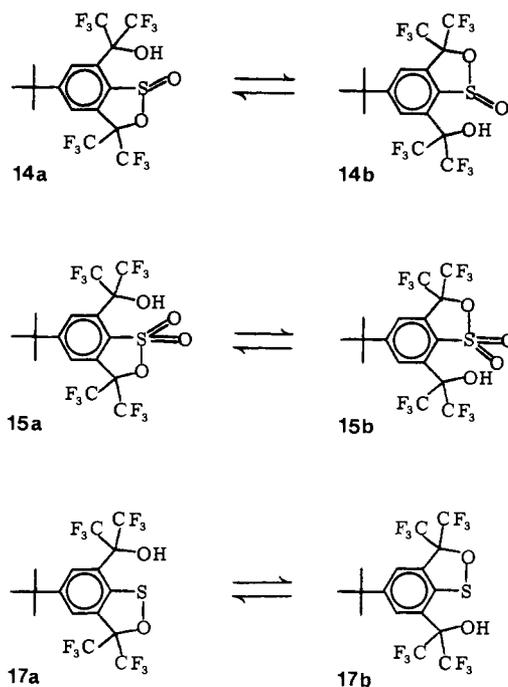
titrated with a NaOH solution (1 × 10^{-2} same solvent) utilizing a standardized glass electrode. The pK_a values for **14**, **15**, and **17** respectively were 5.0, 7.2, and 4.4. The glass electrode was standardized immediately prior to use by titrating propionic acid (pK_a 4.9) for the titration of **14**, p-nitrophenol (pK_a 7.2) for **8**, and 2,4-dinitrophenol (pK_a 4.0) for **17**.[11]

Results

Syntheses. Syntheses of **1–3** are outlined in Scheme II. The conversion of amino alcohol **11**[8] to oxathiane **12** was carried out, without isolation of any intermediary products, in 70% overall yield. The addition of TMEDA was required, along with n-butyllithium, to effect lithiation ortho to sulfur in **12**. The addition of HFA converted virtually all of the lithiated oxathiane **12** to **13**. Oxidative deprotection of **13** was readily accomplished by reaction with NBS. The conversion of **14** to title compounds **1–3** was accomplished in the straightforward manner shown in Scheme II.

Temperature Dependence of NMR Spectra. In all three title compounds (**1–3**), the low-temperature NMR data are consistent with the closed structures depicted. The 85 °C 220-MHz ^{1}H NMR spectra of **1–3** show one singlet in the aromatic region. The 338-MHz ^{19}F NMR spectra of **1** and **3** at −90 °C each have one sharp singlet, as expected for the four equivalent CF_3 groups of the illustrated structures. The 338-MHz ^{19}F NMR spectrum of **2** at −90 °C has two quartets, consistent with two equivalent geminal pairs of nonequivalent CF_3 groups.

In contrast, the variable-temperature NMR spectral data of the conjugate acids of **1–3** (acids **15**, **14**, and **17**) are consistent with the dynamic equilibria shown in Scheme III. The separations of ^{19}F NMR singlets in **15** and **17** diminish with an increase in temperature and eventually coalesce to give single peaks. The quartets of **14** change similarly with increasing temperature, going from four quartets to two. The values of $G^*_{25 °C}$ for their degenerate rearrangements, calculated[12] using the data from the near exchange and no exchange regions, are 14 kcal/mol for **15**, 13 kcal/mol for **14**, and 13 kcal/mol for **17**.

Base catalysis of the above interconversion was established by the observation that the 84-MHz ^{19}F NMR spectrum of a 0.1 M solution of **15** in CD_3COCD_3, 0.07 M in pyridine, exhibits only one broad singlet at δ 75.2, indicating a large increase in the rate of equilibration. The base-catalyzed exchange probably proceeds via sulfuranide dioxide anion **1**, the symmetrical conjugate base of **15**.

or
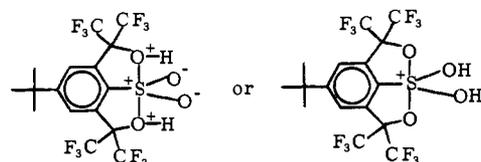
The addition of acid (10 equiv of CF_3SO_3H to a 0.1 M solution of **15** in CH_2Cl_2) resulted in two sharp singlets in the 84-MHz ^{19}F NMR spectrum at δ −75.0 and −75.4, providing no evidence for acid-catalyzed symmetrization mechanisms, which could proceed via one of the symmetrically protonated 10-S-5 species pictured above. The interconversion of **15a** and **15b** is first order in alcohol. The rate constant for the reaction is unchanged over a range of concentrations from 0.1 to 0.001 M (in CH_2Cl_2). This rules out a bimolecular process via a transition state such as the one below.

2 **15a** ⇌ ... ⇌ 2 **15b**
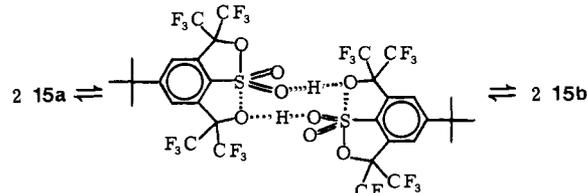
An intramolecular insertion of a sulfonyl S–O bond of **15** into the alcohol O–H bond (to form hydroxysulfurane oxide) could be operative. An analogous process could also account for the equilibration of **14** and **17**.

15a ⇌ [...] ⇌ ... ⇌ **15b**
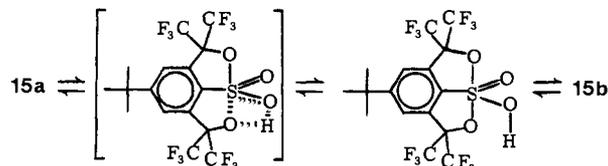
Acidities of the Conjugate Acids of the Hypervalent Anions. The pK_a values at 25 °C for the hypothetical equilibria between alcohols **15**, **14**, and **17** and their conjugate open-chain bases (**18**, **19**, and **20**) were estimated (by using a Hammett $\sigma\rho$ correlation

15 ⇌ ... Et_4N^+ **18**

14 ⇌ ... Et_4N^+ **19**

17 ⇌ ... Et_4N^+ **20**

(11) Hendrickson, J. B.; Cram, D. J.; Hammond, G. S. "Organic Chemistry"; McGraw-Hill: New York, 1970; pp 305–306, 320.

(12) The $\Delta G^*_{25 °C}$ was approximated by using the NMR data from the near exchange region and the Gutowsky–Holm equation : $\Delta\nu_{obsd}/(\Delta\nu_B - \Delta\nu_A) = [1 - \frac{1}{2}\pi^2\tau^2(\nu_B - \nu_A)^2]^{1/2}$. Gutowsky, H. S.; Holm, C. H. *J. Chem. Phys.* **1956**, *25*, 1228.
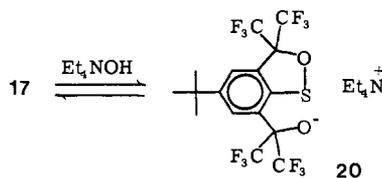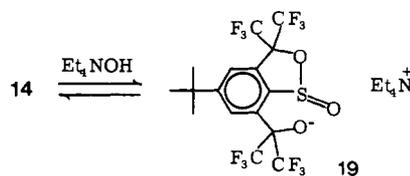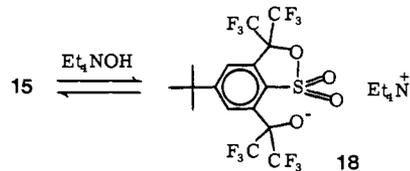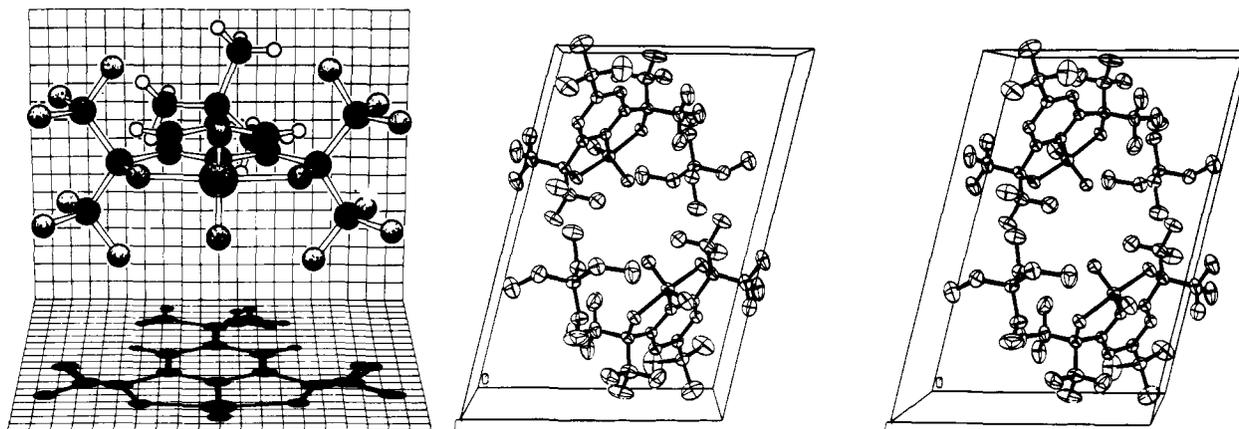
Figure 1. KANVAS plot[14a] and ORTEP[14b] crystal packing diagram of **1**.
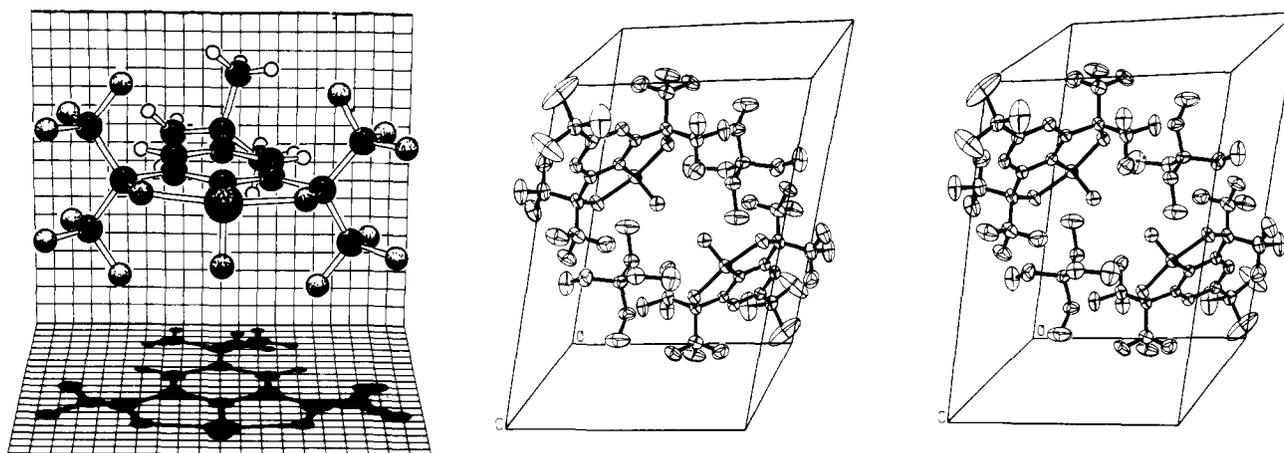
Figure 2. KANVAS plot[14a] and ORTEP[14b] crystal packing diagram of **2**.
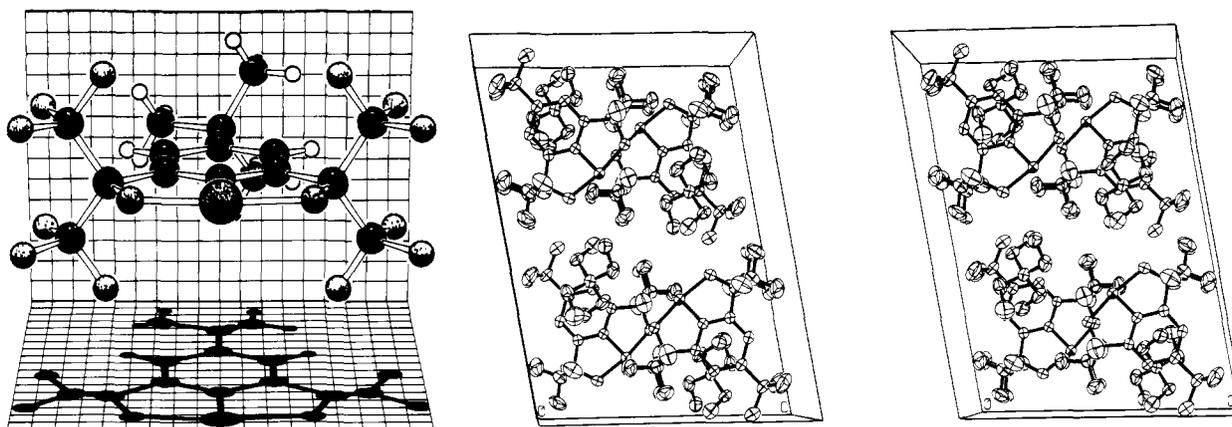
Figure 3. KANVAS plot[14a] and ORTEP[14b] crystal packing diagram of **3**.

determined for the acidity of ring-substituted hexafluorocumyl alcohols) to be 9.1, 9.3, and 9.9, respectively.[13] The lower pK_a values measured titrimetrically for **15** (pK_a 7.2), **14** (pK_a 5.0), and **17** (pK_a 4.4) imply that in solution the closed symmetric

structures **1**, **2**, and **3** are 2.6, 5.9, and 7.5 kcal/mol lower in energy ($\Delta G_{25\,°C}$) than their unsymmetrical (open-chain) isomers **15a**, **14a**, and **17a**.

X-ray Structures. Figure 1 shows the KANVAS[14a] plot (which includes shadow plane, back plane, and a shadow projection) and the ORTEP[14b] crystal packing diagram of **1**. Figure 2 shows the

---

(13) The pK_a values were calculated by applying estimated Hammett σ values for the ρ value (+1.1) determined for measured acidities of substituted hexafluorocumyl alcohols. For all three estimates the σ_m value for $C(CH_3)_3$ (−0.06) and σ_m for $C(CF_3)_2OH$ (0.35) (obtained from Sheppard, W. A.; Sharts, C. M. "Organic Fluorine Chemistry"; Benjamin: New York, 1969) were applied. The σ_p values for $SOCH_3$ (0.17), $S(O)OCH_3$ (0.73), and $S(O)_2OR$ (0.90) were used to approximate values of σ for the ortho sulfur moieties in **17**, **14**, and **15**, respectively. Chapman, N. B.; Shorter, J. "Correlation Analysis in Chemistry"; Plenum: New York, 1969. Some of the preliminary Hammett studies were carried out by M. R. Ross using 50% v/v ethanol/H_2O at 25 °C. Ross, M. R. Ph.D. Thesis, University of Illinois, Urbana, IL, 1981.

(14) (a) Using the coordinates from the X-ray crystallographic analysis the KANVAS program plots a shaded ball and stick model, perpendicular back and shadow planes, and a shadow projection. The spacing between the grid lines represents 0.5 Å. In the above plots the light source is normal to the plane of the phenyl ring. This program is based on the program SCHAKAL of E. Keller (Kristallographischer Institut der Universitat Freiburg, FRG), which was modified by A. J. Arduengo III (University of Illinois, Urbana) to produce the back and shadowed planes. (b) Johnson, C. K. ORTEP II: A fortran thermal ellipsoid plot program, ORNL-3793, Oak Ridge National Laboratory, Oak Ridge, TN, 1971.

KANVAS plot and crystal packing diagram of **2**, and Figure 3 shows the KANVAS plot and crystal packing diagram of **3**. Selected bond lengths and angles are listed in Table IV.

Discussion

Evidence for Hypervalent Sulfur Anions in Solution: (a) 10-S-3 Sulfuranides. The titrimetrically measured pK_a of sultene alcohol **7** (4.4) is substantially lower than that (9.9) estimated for the hypothetical equilibrium between **17** and its open-chain conjugate

17   **21**

22
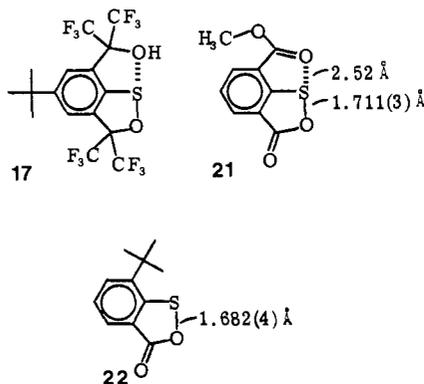
base **20**. This provides unequivocal evidence for stabilization of the anion by bridging to form a 10-S-3 sulfuranide anion in solution. A Hammet $\sigma\rho$ treatment is formally applicable only for meta and para substituents for which through-space interactions with the reaction center are negligible. The use of the σ_{para} substituent constant as an approximation for the expected substituent effect for an ortho substituent, therefore, assumes that the through-space interactions are energetically equal in the acid and its conjugate base. The discrepancy between the actual (4.4) and the estimated (9.9) pK_a values for **17**, a difference of 5.5 pK_a units, implies a through-space stabilizing interaction 7.5 kcal/mol greater for the hypervalent anion than for the acid. This allows a lower limit to be set for the magnitude of the stabilization of the hypervalent anion (relative to its hypothetical unsymmetrical isomer **20**) of 7.5 kcal/mol.

The X-ray structural analyses of **21**[15] and **22**[16] indicate a substantial intramolecular interaction (of the type we suspect in **17**) between sulfur and oxygen in **21**. The very short (2.52 Å) distance (compared to the sum of van der Waals radii (3.25 Å)) between the carbonyl oxygen and sulfenyl sulfur in **21**, coupled with the elongation of the endocyclic sulfur carboxylate oxygen bond (1.711 Å) compared to **22** (1.682 Å) is compelling evidence for this through-space interaction.

The effect of such an interaction in **17** would be to lower its energy compared to that expected for an identically substituted hexafluorocumyl alcohol without such through-space interaction. The estimated pK_a for the hypothetical equilibrium between **17** and **20** then represents a value that is probably underestimated. In Figure 4 this could be represented by moving both **17** and **20** up in energy relative to **3**, thus increasing the energy gap between **20** and **3**.

Evidence for the existence of two other 10-S-3 species has been reported by Lau.[17a] The anion of salt **23** was shown to exist in

23   M = K, Et₄N   **24**   **25**
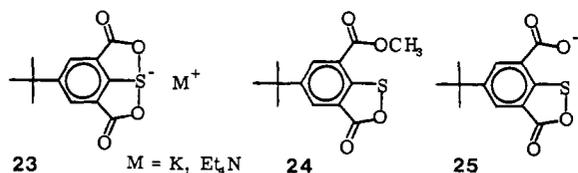
the ground state as a closed structure.[17a,b] There is only one

(15) Krische, B.; Walter, W.; Adiwidjaja, G. *Chem. Ber.* **1982**, *115*, 3842.
(16) Walter, W.; Krische, B.; Adiwidjaja, G.; Voss, J. *Chem. Ber.* **1978**, *111*, 1685.
(17) (a) Lau, P. H. W.; Martin, J. C. *J. Am. Chem. Soc.* **1978**, *100*, 7077. (b) Lau, P. H. W. Ph.D. Thesis, University of Illinois, Urbana, IL 1979.

Table IV. Structural Data for 1–3 and Related Compounds

structure		bond distance, Å	angle,[a] deg	ref
1	a	1.912 (2)	ab, 192.31 (9)	this work
	b	1.930 (2)	cd, 117.8 (1)	
	c	1.772 (3)	de, 122.7 (1)	
	d	1.426 (2)	ac, 84.4 (1)	
	e	1.417 (2)	bc, 83.4 (1)	
			ad, 92.9 (1)	
			ae, 93.7 (1)	
			bd, 92.4 (1)	
			be, 92.8 (1)	
2	a	1.969 (3)	ab, 194.1 (1)	this work
	b	1.969 (3)	cd, 109.5 (2)	
	c	1.790 (4)	ad, 94.7 (2)	
	d	1.483 (4)	bd, 94.5 (2)	
			ac, 83.8 (2)	
			bc, 83.1 (1)	
3	a	1.900 (3)	ab, 189.5 (1)	this work
	b	1.965 (3)	ac, 85.4 (2)	
	c	1.724 (4)	bc, 85.1 (2)	
31	d	1.437 (3)	cd, 108.7 (2)	19
	c	1.806 (3)	ac, 89.8 (1)	
	a	1.684 (3)		
32	a	1.780 (5)	ab, 187.7 (2)	21
	b	1.777 (5)	cd, 117.7 (3)	
	c	1.784 (5)	ae, 94.3 (2)	
	d	1.796 (6)	ac, 87.4 (2)	
	e	1.439 (4)	bd, 87.2 (2)	
33	a	1.819 (5)	ab, 182.9 (2)	21
	b	1.832 (5)	cd, 108.1 (4)	
	c	1.803 (7)	ac, 85.8 (4)	
	d	1.798 (8)	bd, 87.2 (3)	
34	a	1.627 (8)		22
	d	1.411 (8)	de, 118.9 (1.2)	
	e	1.421 (8)		
	c	1.791 (11)		
35	a	1.60	ac, 92	25
	c	1.77	ad, 108	
	d	1.45	cd, 106	
36	c	1.765		26
	d	1.446		
37	c	1.808 (4)		27
38	c	1.802 (2)		28
39	a	1.878 (2)	ab, 183.9	29
	b	1.879 (2)	ac, 88.3	
	c	1.720 (2)		

[a] For 10-S-3 and 10-S-4 species ∠ab is defined as the angle between bond a and b whose arc includes the sulfur lone pair. For 10-S-5 the arc of ab includes either an equatorial oxygen (for **32**) or the bisector of the O–S–O angle in the equatorial plane (for **1**).

Figure 4. Relative energy levels of **3**, **17**, and **20**.

carbonyl stretching frequency (1638 cm^{-1}) in the IR spectrum of **23**. In contrast, two distinct $\nu_{C=O}$ stretching frequencies are observed in the IR spectrum of **24** (C=O peaks at 1736 and 1670 cm^{-1}). While NMR evidence cannot rule out rapidly equilibrating structures such as **25** and **26a**, the short time scale of infrared


26a   **26b**   **27**   M = K, Et$_4$N
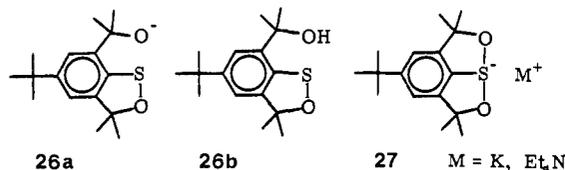
spectroscopy (10^{-13} s) makes the observation of a single carbonyl stretching frequency in **23** convincing evidence for the depicted symmetrical sulfuranide structure. The pK_a of **26b**[17b] is somewhat lower than the pK_a of *tert*-butyl alcohol,[18] indicating that the closed structure **27** may be the ground state for this species.

(b) 10-S-4 Sulfuranide Oxides. The anion of **2** is the first 10-S-4 sulfuranide oxide anion for which unequivocal evidence has been obtained. The sultine alcohol **28**, an analogue of **14** with CF$_3$

28   **29**
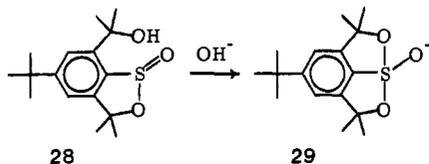
groups replaced by CH$_3$ groups, was described earlier.[17a] Its NMR spectra reflect structural features for the unsymmetrical alcohol and its symmetrical conjugate base parallel to those described for the trifluoromethyl analogue **14**. This case as well the apparent symmetry evidenced by the NMR spectrum of the anion could either be the consequence of a closed-ring sulfuranide oxide ground state (such as **29**) or a low-energy barrier for interconversion of open-chain sultine alkoxides **30a** and **30b**. The fact that the

30a   **30b**

titrimetrically measured pK_a of **14** (5.0) is substantially lower than that (9.3) estimated for the hypothetical equilibrium between **14** and its open-chain conjugate base **19**, provides evidence for a 10-S-4 sulfuranide oxide anion in solution. An energy diagram analogous to Figure 4 (drawn for the sulfur(IV) analogues) would show a minimum energy difference between **2** and **19** of 6.3 kcal/mol. In this case as well, the X-ray crystallographic data for the structurally similar **31**[19] provide evidence for the intramolecular through-space interaction shown. The intramolecular sulfenyl sulfur to carbonyl oxygen, S–O, distance (2.81 Å) is substantially shorter than the sum of the van der Waals radii (3.25 Å). Although this suggests through-space unsymmetrical hypervalent bridging to sulfur in **31**, the interaction is not as strong

31   **14**
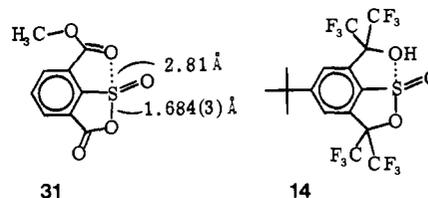
as the through-space S–O interaction of **21** (r_{S-O} = 2.52 Å). The intramolecular S–O bridging apparent in structures **21** and **31** makes it seem likely that there is a ground-state interaction between the sulfur and the O–H oxygen in sultine alcohol **14**, albeit weaker than that in sultene alcohol **17**. The effect of bridging in **14** is to lower the energy of **14** and **2** relative to **19**; 6.3 kcal/mol is therefore a lower limit estimate of the energy gap between open anion **19** and closed anion **2**.

(c) 10-S-5 Sulfuranide Dioxide 1. The sulfuranide dioxide **1** is the first example of a 10-S-5 single-minimum ground-state anion. The application of arguments parallel to those presented in the above discussion of pK_a values of sultene alcohol **17** and sultine alcohol **14** to the difference between the measured pK_a (7.2) and the calculated pK_a (9.1) of sultone alcohol **15** leads to the conclusion that hypervalent structure **1** is at least 2.6 kcal/mol more stable than its open-chain isomer **18**. Although the spacings are quantitatively different, the relative order of energy levels for **1**, **15**, and **18** is the same as in Figure 4.

The energetic preference for the hypervalent structure, relative to its open-chain isomer is therefore less for **1** than for **2**, and less for **2** than for **3**.

The pK_a evidence from each of the three studies is consistent with either a single-minimum ground state or an unsymmetrically bridged anionic ground state in solution, with substantial hypervalent stabilization relative to the unbridged species. Evidence for the symmetrical, single-minimum structures for **1–3** was obtained by X-ray crystallography (see below).

Significance and Implications of the Geometries of 1–3 in the Solid State. Structures of the novel 10-S-5 sulfuranide dioxide anion **1**, 10-S-4 sulfuranide oxide anion **2**, and 10-S-3 sulfuranide **3** have been elucidated by X-ray crystallographic analysis.

The geometry about 10-S-5 sulfur in **1** is approximately TBP. The equatorial angles ($\angle$cd and $\angle$de, see in Table IV)[20] deviate from the ideal 120° by less than 3°. The apical O–S–O bond angle ($\angle$ab) is bent ca. 12° from the ideal 180° (with deformation of the O–S–O bond in the direction of the phenyl ring and away from the equatorial oxygen atoms). Two factors are thought to be responsible for the deviation of the apical O–S–O bond from linearity: (1) the repulsive interaction of the nonbonding electrons on the equatorial oxygens and the apical bonds[21] and (2) the ring strain inherent in two bridged five-membered rings.

The equatorial S–O bonds ($\sim$1.42 Å) of **1** are similar in length to the sulfonyl S–O bonds of **34**[22] ($\sim$1.42 Å). The change of

---

(18) The pK_a of **26b**, measured in Me$_2$SO,[17b] was found to be comparable to the pK_a of H$_2$O (27.5) in Me$_2$SO. The pK_a of *tert*-butyl alcohol measured in Me$_2$SO is 1.9 pK_a units higher (29.4). The values for H$_2$O and *tert*-butyl alcohol are from: Arnett, E. M.; Small, L. E. *J. Am. Chem. Soc.* **1977**, *99*, 808.

(19) Walter, W.; Krische, B. Adiwidjaja, G. *Leibigs Ann. Chem.* **1980**, 14.

(20) The letters in parenthesis in the following discussion refer to the bond lengths and angles labeled in Table IV.

(21) For a fuller discussion of the deviation from linearity of O–S–O bonds in the structurally similar **32** and **33**, see: Perozzi, E. F.; Martin, J. C.; Paul, I. C. *J. Am. Chem. Soc.* **1974**, *96*, 6735.

hybridization from sp^3 to sp^2 on going from **34** to **1** might be expected to make the equatorial S–O bonds shorter, offsetting the bond elongation expected to result from the introduction of net negative charge on **1**.

The distorted ψ-TBP geometry around 10-S-4 sulfur in **2** shows an equatorial C–S–O bond angle ($\angle cd$) of 109.5°, in the range of 10-S-4 sulfuranes.[23] The apical O–S–O angle ($\angle ab$) in **2** is distorted from colinearity, more (14°) than the corresponding angle ($\angle ab$) in **1** (12°). These increased distortions from ideal geometry seen in **2** compared to **1** are in the direction predicted by valence shell electron pair repulsion (VSEPR) theory.[24] These geometric differences can also be thought of as concomitant features of the difference in hybridization of the sulfur orbitals in **1** vs. those of **2**. There is an energetic advantage to increasing the s character of a lone pair. Compared to **1**, therefore, the lone pair of **2** has more s character while the C–S(c) and S–O(d) equatorial bonds include more p character. This makes the C–S–O ($\angle cd$) bond angle smaller in **2** and, perhaps, slightly elongates the equatorial bonds (C–S(c) and S–O(d)). This trend is also seen when **33** is compared to **32**.[21] The equatorial C–S bonds (c and d) are slightly longer while the equatorial C–S–C angle ($\angle cd$) is smaller in **33** and **32**.

The sulfoxide S–O bond (d) length of sultine **35**[25] is somewhat shorter than the equatorial S–O bond (d) length of sulfuranide oxide **2**. Just as **1** might have been expected to have longer equatorial S–O bonds (d and e) than those of sulfonate ester **34** (because of the full negative charge on **1**) one might also expect **2** to have a longer equatorial S–O bond (d) than that of sulfinate ester **35**. Unlike the former comparison, however, there is no apparent offsetting increase in the amount of s character expected in the contributing sulfur orbitals of the S–O bonds (d) of **2** compared to **35**. Hypervalent bridging to sulfinyl sulfur therefore results in elongation of the equatorial S–O bond (d) in **2**, while this equatorial S–O bond elongation is not observed as a result of hypervalent bridging to sulfonyl sulfur in **1**.

An even closer analogue to sulfuranide oxide **2**, sulfinic anhydride **31**,[19] has an even shorter exocyclic S–O bond (d) than **35**. Here also sulfur appears to employ an sp^3 hybridized orbital in bonding to sulfoxide oxygen, which may be inferred from the 108.7° C–S–O angle ($\angle cd$).

The geometry of 10-S-3 sulfur in sulfuranide **3** is also ψ-TBP. The exocyclic apical O–S–O angle ($\angle ab$) is 189.8°, somewhat nearer to 180° than those of **1** and **2**. The shorter C–S bond (c) of **3** (compared to that of **1** or **2**) allows the apical O–S–O bond to more closely approach the ideal 180° angle with less ring strain from the two bridging five-membered rings. The C–S bond lengths (c) in sulfones (e.g., **36**)[26] are shorter than those in sulfoxides (**37**)[27] or sulfides (**38**),[28] probably the result of increased effective positive charge on sulfur. The C–S bond lengths are about equal in sulfoxides (e.g., **37**) and sulfides (**38**). The same trend is followed in the first two members of the series **1**, **2**, and **3**. The C–S bond (c) length in sulfuranide oxide **2** is longer than the C–S bond (c) in sulfuranide dioxide **1**. The C–S bond (c) length of sulfuranide **3** (the next member of the series) is, however, much shorter than the C–S bond (c) of **2**. (1.724 vs. 1.790 Å). The fact that the lengths of the C–S bonds (c) in the hypervalent series do not parallel the trend seen in the sulfone–sulfoxide–sulfide series may be the consequence of substantial double-bond character in the C–S bond (c) of **3**, causing it to be much shorter than those of **2** or **1**. There is no such possibility in the comparisons of **38** vs. **37** or **36**.

In the structurally similar dioxathiapentalene **39**,[29] frequently drawn with a double bond between sulfur and carbon, the C–S bond length is almost identical (1.720 Å) with that of **3** (1.724 Å).

Delocalization of negative charge into the aromatic ring of **3** requires C–S double-bond character. The increase in negative charge in the aromatic ring resulting from such delocalization is expected to cause upfield chemical shifts of some ring atoms in **3**. Peaks for the aromatic protons meta to the sulfur are found at substantially higher field in **3** (7.4 ppm) than in **2** (7.8 ppm) or **1** (7.8 ppm). The chemical shifts of the aromatic ring carbons para to the sulfur in the ^{13}C NMR spectra of **1** (160.1 ppm), **2**, (157.4 ppm), and **3** (150.2 ppm) also demonstrate the expected higher upfield shift (in the para ring carbon of **3** compared to **2** or **1**).

Another noteworthy structural feature of **3** is the rather large difference in apical S–O bond lengths (0.066 Å). This polarization may be ascribed to steric repulsion between the unsymmetrically positioned tetraalkylammonium counterion and the oxygen of the shorter of the two S–O bonds (see Figure 3). The proximate ethyl carbon is only 3.029 (9) Å from the oxygen of the shorter S–O bond. Hypervalent bonds are known to be easily deformable (and highly polarizable).[30] The small deformations from the ideal symmetrical hypervalent structures which are observed for **1** and **3** are therefore reasonably ascribed to the effects of crystal packing forces. It is most reasonable to consider **1–3** to be symmetrical structures with single energy minima for the O–S–O hypervalent bond.

Comparisons of Nucleophilic Attack at Sulfonyl, Sulfinyl, and Sulfenyl Sulfur. Since the energy differences between **1** and **18** is approximately 2.6 kcal/mol, between **2** and **19** is approximately 5.9 kcals/mol, and between **3** and **20** is approximately 7.5 kcals/mol, one might expect nucleophilic displacement at sulfonyl sulfur to be slower than at sulfinyl sulfur, which, in turn, should be slower than those at sulfenyl sulfur.[48] According to Kice:[31] "Qualitatively it has been recognized for some time that nucleophilic substitution at sulfenyl sulfur is more rapid than at sulfinyl sulfur, and that substitution at the latter is more rapid than substitution at sulfonyl sulfur".

Ligand Design and Reaction Rates. The tridentate ligand used in preparation of the title compounds has been used in preparation of other novel compounds of hypervalent bromine and iodine.[32] The features that were built into the tridentate ligand in order to stabilize TBP relative to Td geometries have been discussed.[32,33] Some of these features have been identified through relative rate studies. The presence of an equatorial–apical five-membered ring is one of the important structural features of this ligand design. The rate of hydrolysis of cyclic sulfate and sulfinate esters with five-membered rings is much faster than that of their open chain analogues.[2o,p] The same dramatic difference in reaction rates is observed between the intramolecularly catalyzed hydrolysis rates of sulfonamides such as **40**, which may proceed via a five-membered ring transition state (**41**), and hydrolysis rates of sulfonamides such as **42**, which cannot do so.[34]

Another feature of our ligand system expected to stabilize the TBP geometry is the Thorpe–Ingold *gem*-dialkyl effect.[35] Intramolecularly catalyzed hydrolyses of sulfonamides with neighboring nucleophilic groups have been shown[36] to proceed with rates that increase with increasing bulk of *gem*-dialkyl substituents

(22) Fleischer, E. B.; Kaiser, E. T.; Langford, P.; Hawkinson, S. Stone, A.; Dewar, R. *Chem. Commun.* **1967**, 197.

(23) Martin, J. C.; Perozzi, E. F. *Science (Washington, D.C.)* **1976**, *191*, 154.

(24) (a) Gillespie, R. J.; Nyholm, R. S. *Q. Rev., Chem. Soc.* **1957**, *9*, 339. (b) Gillespie, R. J. *Can. J. Chem.* **1960**, *38*, 818.

(25) Surcouf, E. *Acta Crystallogr., Sect B* **1979**, *B35*, 1922.

(26) Langs, D. A.; Silverton, J. V.; Bright, W. M. *J. Chem. Soc. D* **1970**, 1653.

(27) Typke, V. *Z. Naturforsch., A* **1978**, *33A*, 842.

(28) Dreizler, H.; Rudolf, H. D. *Z. Naturforsch., A* **1962**, *17A*, 712.

(29) Gilardi, R. D.; Karle, I. L. *Acta Crystallogr., Sect. B* **1971**, *B27*, 1073.

(30) Lam, W. Y.; Duesler, E. N.; Martin, J. C. *J. Am. Chem. Soc.* **1981**, *103*, 127.

(31) Kice, J. L. *Prog. Inorg. Chem.* **1972**, *17*, 147.

(32) Nguyen, T. T.; Amey, R. L.; Martin, J. C. *J. Org. Chem.* **1982**, *47*, 1024.

(33) Nguyen, T. T.; Wilson, S. R.; Martin, J. C. *J. Am. Chem. Soc.*, submitted for publication.

(34) Wagenaar, A.; Kirby, A. J.; Engberts, J. B. F. N. *Tetrahedron Lett.* **1974**, 3735.

(35) (a) Beesley, R. M.; Ingold, C. K.; Thorpe, J. F. *J. Chem. Soc.* **1915**, *107*, 1080. (b) Ingold, C. K. *Ibid.* **1921**, *119*, 305.

(36) Jager, J.; Graafland, T.; Schenk, H.; Kirby, A. J.; Engberts, J. B. F. N. *J. Am. Chem. Soc.* **1984**, *106*, 139.

40

41

42
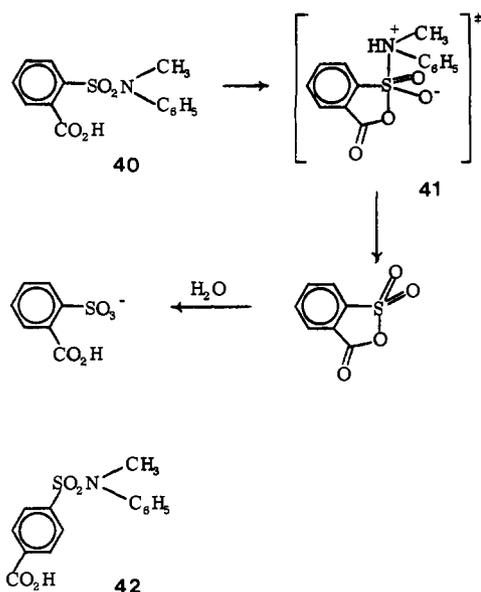
adjacent to the sulfonyl sulfur, consistent with a cycle 10-S-5 transition state.

The effectiveness of the tridentate ligand of **43** is dramatized

43, X = Br, I, S⁻, SO⁻,
SO₂⁻, IO, IF₂
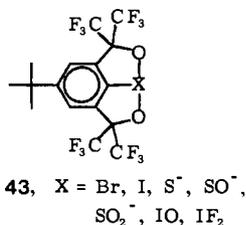
by characterizing the tridentate ligand as a host and the nonmetal X as a guest, using the nomenclature of Cram.[37] The host is

geometrically constrained to have almost the same geometry as it does in the host–guest complex, thus minimizing disadvantageous entropic factors in the formation of the complex while all the enthalpic advantages of the bonds around the central atom add to its stability. The host exerts a viselike grip on his guest.

The existence of 10-S-3 sulfuranides, 10-S-4 sulfuranide oxides, and 10-S-5 sulfuranide dioxides as single energy minimum ground-state structures indicates that other 10-S-3, 10-S-4, and 10-S-5 species may be energetically stable enough to exist as intermediates. It does not, however, prove the existence of an intermediate in any particular associative nucleophilic reaction at sulfur, except the ones forming **1–3**.

(37) Cram, D. J. *Science (Washington, D.C.)* **1983**, *219*, 1177.

Heavy-Atom Kinetic Isotope Effects in the Acid-Catalyzed and Thermal Rearrangements of 2,2'-Hydrazonaphthalene. Transition-State Differences in Their Concerted Rearrangements[1]

Henry J. Shine,*[†2] Ewa Gruszecka,[†3] Witold Subotkowski,[†] Marilyn Brownawell,[‡] and Joseph San Filippo, Jr.[‡4]

Contribution from the Departments of Chemistry, Texas Tech University, Lubbock, Texas 79409, and Rutgers University, New Brunswick, New Jersey 08903. Received November 16, 1984

Abstract: Acid-catalyzed (70% aqueous dioxane at 0 °C) and thermal rearrangement (95% ethanol at 80 °C) of 2,2'-hydrazonaphthalene (**1**) into 2,2'-diamino-1,1'-binaphthyl (**2**) have been shown to be concerted, [3,3]-sigmatropic shifts. This was accomplished by measuring the nitrogen and carbon kinetic isotope effects (KIE), for which purpose mixtures of **1** with [¹⁵N,¹⁵N']**1** and [1,1'-¹³C₂]**1** were used. KIE were calculated from whole-molecule mass ratios, measured by multiscan mass spectrometry, in the bis(trifluoroacetyl) derivative of product **2**, isolated after low and high conversions. The results (averaged) were, for two isotopic atoms, $k(^{14}N)/k(^{15}N) = 1.0904$, $k(^{12}C)/k(^{13}C) = 1.0086$ in the one-proton, acid-catalyzed rearrangement and 1.0611 and 1.0182, respectively, in the neutral, thermal rearrangement. These results indicate that although the rearrangements are concerted processes, the breaking of the N–N bond and the forming of the C–C bond proceed to different extents in the transition states. Furthermore, the difference in the timing of these events is greater in the acid-catalyzed than in the thermal rearrangement, a difference which may be attributable to earlier C–C bonding in the polar transition state of the former.

Among benzidine rearrangements[5-15] those of hydrazoarenes which contain the 2-naphthyl group constitute a unique class. First, in acid-catalyzed rearrangements in the usual solvents

(aqueous ethanol or aqueous dioxane), they undergo almost complete *o,o'*-bonding with little or no concommitant dispro-

(1) Previous paper: Shine, H. J.; Park, K. H.; Brownawell, M.; San Filippo, J., Jr. *J. Am. Chem. Soc.* **1984**, *106*, 7077.